

Pitting Corrosion Evaluation of Titanium in NH_4Br Solutions by Electrochemical Methods

R. Ittah*, E. Amsellem and D. Itzhak

Department of Materials Engineering, Ben-Gurion University of the Negev, Beer-Sheva, Israel

*E-mail: ittahr@bgu.ac.il

Received: 30 August 2013 / Accepted: 12 October 2013 / Published: 8 December 2013

Anomalous pitting sensitivity of titanium in ammonium bromide solutions was detected. Under saturation conditions pitting was not observed visually after anodic polarization and positive hysteresis loop was not recorded. Electrochemical impedance spectroscopy (EIS) shows an increase in resistance with time without an inductive element in the equivalent electrical circuits. This anomalous behavior may be related to changes in the molecular structure of the OH^- bonds under saturation. In dilute ammonium bromide solutions, a pitting attack was observed visually after anodic polarization and cyclic polarization had shown a positive hysteresis loop. EIS shows an inductive loop related to the active pits that exist on the anodic surface.

Keywords: Titanium, pitting, Ammonium Bromide, saturation, EIS, polarization.

1. INTRODUCTION

Titanium and titanium alloys are attractive metallic materials widely used in medicine, dentistry, and aeronautical applications due to their corrosion resistance, mechanical properties/density ratio, and biocompatibility [1-3]. Titanium and its alloys present a high corrosion resistance even in aggressive environments such as halide solutions, because of spontaneous formation of a chemically stable thin passive titanium dioxide (TiO_2) film. According to the literature, titanium alloys are extensively used in bromine production plants, wet chloride media, and diluted or concentrated chloride and bromide environments [4].

A previous study reported that titanium exhibits a much greater sensitivity to localized corrosion in bromide compared to chloride environments [5]. This behavior is attributed to a significant decrease in the anodic breakdown potential under bromide environments [6,7]. The phenomenon was also related to the higher polarizability of bromide compared to chloride ions. Therefore, bromide ion is a better electron donor compared to chloride, enhancing a higher electrical

conductivity of the passive film. Hou and Meng suggested that pit initiation of unalloyed titanium in bromide solutions is related to the absorption of Br^- at the oxide/solution interface, which eventually forms bromide nuclei such as TiBr [8]. It is suggested elsewhere that in bromide media a surface defect in the metal matrix encouraged localized growth of the passive film [9]. These defects appear as an area for a pit nucleus at which a halide ion mass transfer occurs and favoring the formation of titanium tetrahalide or oxyhalide.

Electrochemical studies based on electrochemical impedance spectroscopy (EIS) suggested a relationship between spectra features and pitting steps such as: incubation, propagation, and relaxation. According to these studies, in the early stage of the pitting pathway an inductive loop had been observed under low frequencies, indicating the incubation stage [10]. The propagation of the pitting process as a result of a longer period of exposure is usually characterized by a shift of the extreme in the Nyquist diagram to the direction of the origin (leftward). When the pits became electrochemically inactive the inductive loop disappeared and two capacitive loops could be observed [11]. The first capacitor is related to the passive layer and the second is related to the new interface created by the pitting activity [12,13]. The time of relaxation τ in the pitting process is expressed by:

$$\tau \propto \frac{1}{w^*}$$

Where w^* is the value of the frequency in the minimum of the inductive loop. Lower frequencies indicate longer time of relaxation [14].

Aqueous concentrated bromide solutions are commonly used as electrolytes in electrochemical machining of titanium, and due to their high density they are also used as fluids in the oil drilling process [15,16]. Few studies deal with the behavior of concentrated brines as well as saturated brines as electrolytic media or as corrosion environment [17]. The molecular structure of such media has been studied by Raman spectroscopy [18]. The lack of H_2O molecules in the concentrated brine solutions leads to a change in the OH bonds, which further modifies the chemical activity of the concentrated solutions and may lead to unexpected results.

This article deals with the full spectrum of concentration from 1M of ammonium bromide to the saturated solution at ambient conditions, containing 7M ammonium bromide. Blasco et al. investigated the behavior of titanium in concentrated LiBr solution that is used in absorbing air conditioning machines [19]. They found that the pitting corrosion susceptibility of titanium increased with the LiBr concentration. Madore and Landolt studied the electrolytic polishing of titanium in 5M NH_4Br solution at 25°C [15]. They reported that at 2V vs. $\text{Hg}/\text{Hg}_2\text{SO}_4$ reference electrode, pitting dissolution occurred and the surface became rough. A smooth surface was obtained at potentials above 5 V vs. $\text{Hg}/\text{Hg}_2\text{SO}_4$. In their study, cyclic polarization measurements or EIS were not reported and the main findings were related to the electrochemical machining of titanium as a photoresist.

Titanium, as a passive metal, is usually attacked in localized corrosion such as pitting or crevice formation [4,20]; This sensitivity is augmented by the presence of bromide ions in aqueous solutions. However, in alcoholic media it may result in stress corrosion cracking SCC [21,22]. The present research evaluates the pitting sensitivity of titanium grade 2 in NH_4Br aqueous solutions using EIS technique, cyclic polarization measurements, and SEM observations.

2. MATERIALS AND METHODS

The tests were performed in a three-electrode cylindrical cell using platinum as a counter-electrode and standard Ag/AgCl (3.5M KCl) as a reference electrode as shown in Fig. 1. The working electrodes were made from unalloyed titanium grade 2 with maximum content of 0.3wt% Fe, 0.1wt% C, 0.25wt% O, and 0.03wt% N. The area of the working electrode was 4.5cm². The working electrode samples were cut from 2 mm width plate. Prior to exposure, the tested coupons that acted as working electrodes were polished with SiC paper to 500 grit, rinsed with de-ionized water and dried with acetone. The electrochemical cell was designed to stimulate pitting attack combined with crevice development under the Teflon gasket [23]. The apparatus exposes a large area of the working electrode located parallel to the counter-electrode. Both electrodes have the same size. In this cell the electrical field is homogeneous and the direction of the electrical field is perpendicular to the surface exposed to the environment under the anodic conditions. Test solutions contain NH₄Br in the following concentrations: 1 M, 4 M, and saturated solution of 7 M. The aqueous solutions were prepared from commercial solid NH₄Br and de-ionized water. Polarization and AC impedance measurements were carried out on a Versa stat 3 potentiostat system under computer control using V3 studio software. Cyclic potentiodynamic polarization curves were made using a scan rate of 1mv/s. Electrochemical impedance spectroscopy was made using frequency range between 10,000 Hz and 0.01 Hz with 100 μ A RMS amplitude using potentiostatic technique at ambient conditions. The EIS were made on titanium plates exposed in one run and then inspected by SEM. Three samples were used in each solution: passivity at 0.3 V vs. Ag/AgCl and over the break-down potential at 1.4 V vs. Ag/AgCl. EC-Lab® V10.0 software was used to adapt equivalent circuits to the experiments.

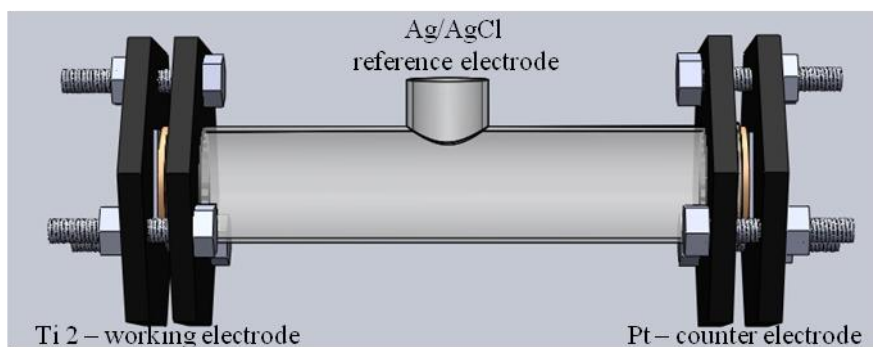


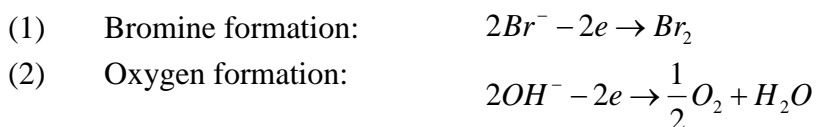
Figure 1. Three electrodes cylindrical cell using for electrochemical tests.

3. RESULTS AND DISCUSSION

The cyclic potentiodynamic polarization results presented in Fig. 2 show monotonic behavior up to 4M bromide and anomalous changes when the content of ammonium bromide reached saturation. The sensitivity to pitting indicated by the positive hysteresis loop increases with changes in the concentration from 1 M to 4 M NH₄Br. Similar behavior could be seen when analyzing the other

parameters presented in Table 1. It can be seen that a minor increase in corrosion rate (equivalent to i_{corr}) was detected when the ammonium bromide content was increased up to 4 M. However, a decrease in the chemical activity was observed during the saturated solution analysis. As a result, Tafel extrapolation, in the polarization diagram, showed a decrease in corrosion rate in the above environment. Cyclic polarization curves in all cases show active-passive transition. The breakdown potential (EBp) in 1 M and 4 M was ~ 1.2 V vs. Ag/AgCl, and the pitting potential (E_{pit}) was about 0.9 V vs. Ag/AgCl. Oscillation in the anodic curve could be seen especially when the scanning started to be cathodic in the range of 1.8–1.6 V vs. Ag/AgCl. This behavior is emphasized in the case of 4 M ammonium bromide, where the pitting sensitivity is very clear. These oscillations indicate instability in the surface composition and the electrical resistivity of the surface.

In the case of saturated solution, the sharp increase in current density at anodic potential of 0.95 V vs. Ag/AgCl is attributed to anodic reactions such as formation of Br_2 or the formation of oxygen as described herein:



The formation of elemental bromine could be clearly seen by a change in the color near the anodic surface and near the Teflon gasket. When this occurs, the anodic potential is equivalent to the redox potential of the bromine formed. It should be emphasized that in all cases anodic polarization above 1.1 V vs. Ag/AgCl induces red-brown color appearance near the anodic surface, meaning the anodic surface became electrically conductive and permitted the oxidation reaction to occur on the surface.

A sharp increase in current density is mainly related to the breakdown of the passive film. The electrical conductivity of the passive film became more significant in the saturated solution and this does not result in pitting features as discussed above as a positive hysteresis loop. Most of the current density causing the formation of bromine and oxygen and the minor part of the current density may be related to anodic dissolution as presented in Fig. 2c. Pitting occurs under 1.4 V in 1 M ammonium bromide solution, unlike the pitting-free surface of titanium grade 2 under 1.4 V in saturated solution. Saturation conditions may lead to unexpected behavior whose chemistry and molecular structure changes are still not sufficiently understood. It can be assumed that during saturation, a lack of H_2O molecules participates in the electrochemical process, which may contribute to the drastic change of the monotonic behavior that was identified in the diluted ammonium bromide solutions. The change in the monotonic feature led to the anomalous behavior of the pitting phenomenon. A new approach to the evaluation of the uses of titanium in the environments containing bromide ions by this anomaly may be suggested. It can also be assumed that similar effects will be detected in other saturated electrolytic solutions that have to be further investigated.

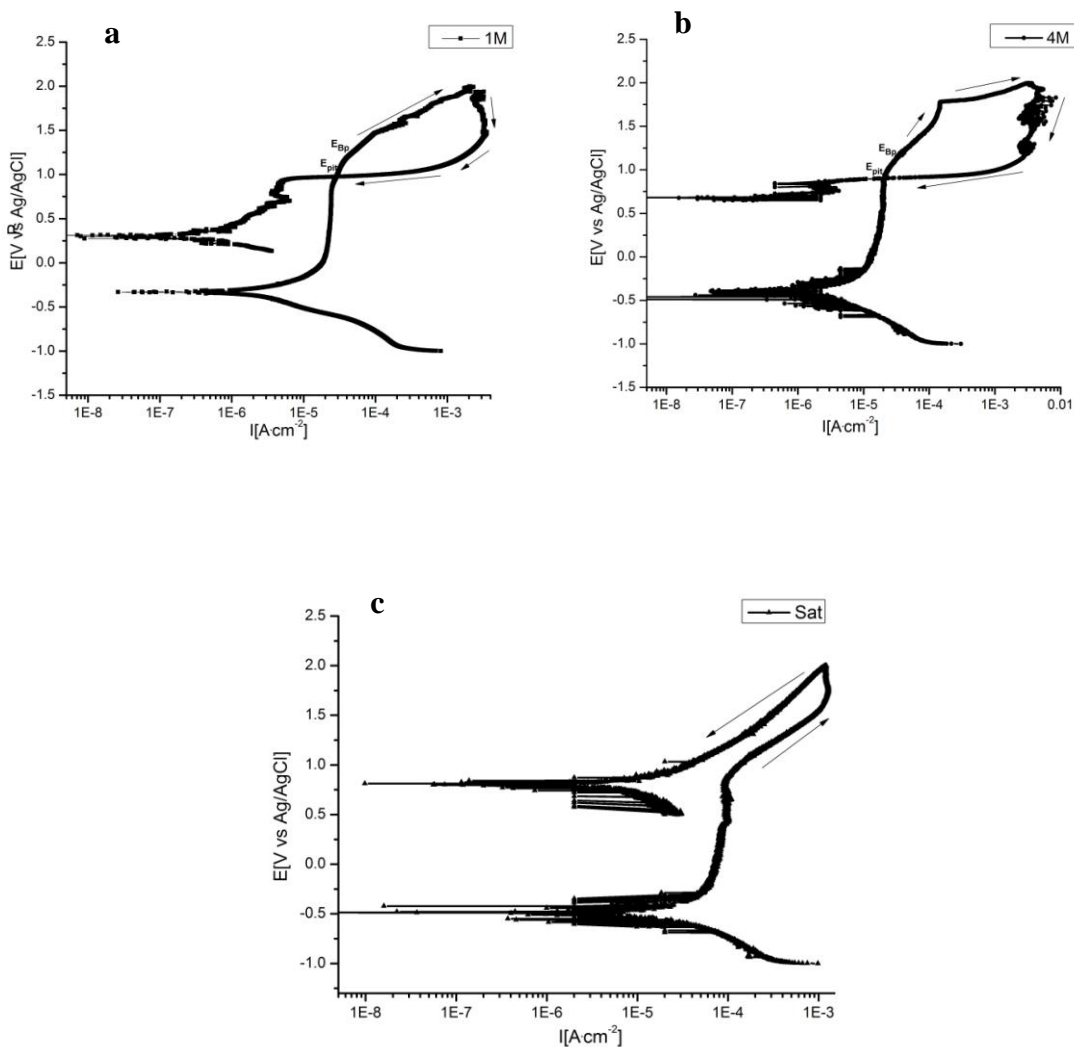


Figure 2. Cyclic potentiodynamic polarization curves for: (a) 1 M NH₄Br (b) 4 M NH₄Br (c) saturate NH₄Br solution

Table 1. Electrochemical corrosion parameters of Ti grade 2 as a function of NH₄Br concentration at ambient temperature

[NH ₄ Br]	<i>E</i> _{corr}	<i>i</i> _{corr}	β_a	β_c	<i>E</i> _{Bp}	<i>E</i> _{pit}
Molar	[mV] vs Ag/AgCl	$\mu\text{A}\cdot\text{cm}^{-2}$	[mV]	[mV]	[mV] vs Ag/AgCl	[mV] vs Ag/AgCl
1	-332.17	2.31	239.86	259.95	1200	980
4	-394.58	2.80	258.91	292.35	1190	900
Saturation	-499.98	1.22	192.90	168.93	--	--

Detailed EIS results are presented in Figs. 3-5 and Tables 2,3. When the anodic potentials were in the passive range, Nyquist diagrams clearly show two semi-circles in all cases (Fig. 3), meaning two capacitors had been detected in the equivalent circuit. The first semi-circle is related to the double

layer capacitor, and the second semi-circle is related to the passive film dielectric material composed of TiO₂. The total impedance was between 80 and 85 kΩ·cm² in all cases as summarized in Table 2.

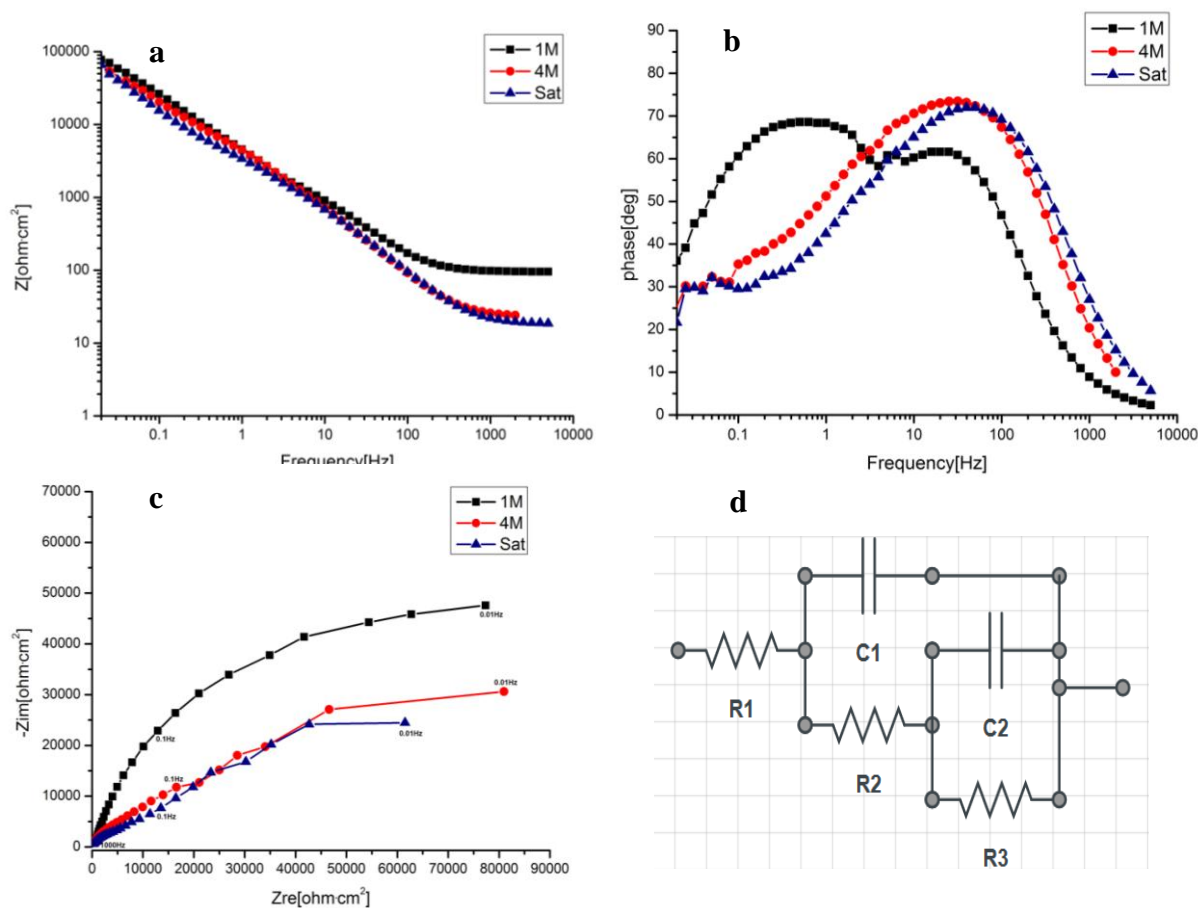


Figure 3. EIS spectra for passivity range of Ti-2 as function of NaBr concentration: (a) Bode diagram (b) bode phase diagram (c) Nyquist diagram (d) equivalent electrical circuit

Table 2. Equivalent circuit parameter for titanium in NH₄Br solutions at passive range (0.3V vs Ag/AgCl)

[NH ₄ Br]	R _s (Ω·cm ²)	C _{dl} [F]	R _p (Ω·cm ²)	C _{p1} [F]	R _{p1} (Ω·cm ²)
1M	115.20	-0.11·10 ⁻³	14751.0	-0.19·10 ⁻³	70857.0
4M	71.55	-0.10·10 ⁻³	7857.0	-0.72·10 ⁻³	76558.0
saturated	46.89	-0.12·10 ⁻³	6592.0	-0.68·10 ⁻³	73408.0

Increasing the anodic potential above the critical value of the current density leads to the appearance of a coil in the EIS analysis. This electrical element is typical of unsaturated and relatively dilute solutions with a concentration up to 4M. Hence, this element was not observed in the saturated solution as shown in Figs. 4,5.

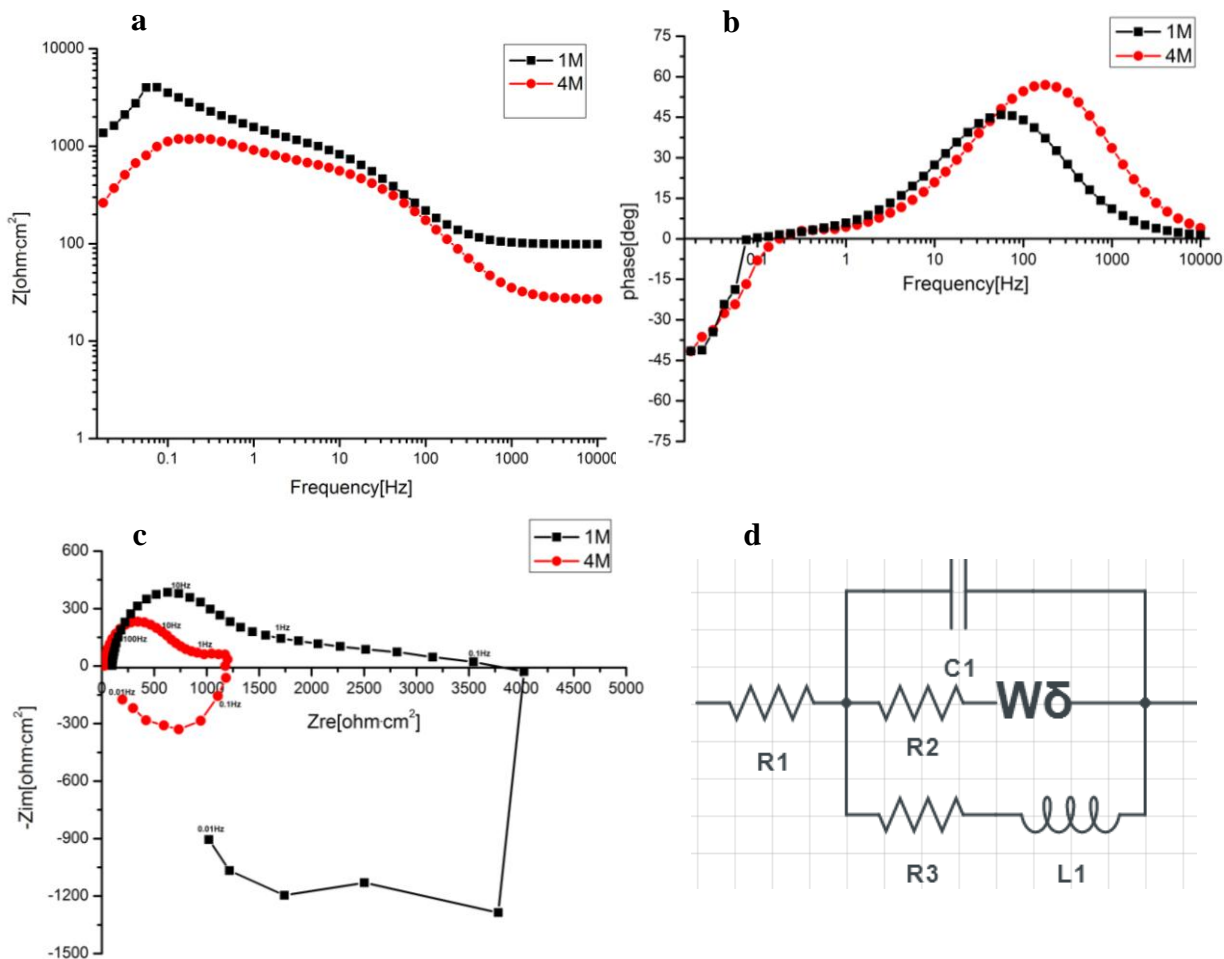


Figure 4. EIS spectra for Ti-2 in 1M and 4M NH₄Br at the transpassive area: (a) Bode diagram (b) Bode phase diagram (c) Nyquist diagram (d) equivalent electrical circuit match to the both of the present concentration.

Table 3. Equivalent circuit parameter for titanium in NH₄Br solutions under anodic potentials higher than the typical breakdown potential (under transpassivity)

[NH ₄ Br]	R _s (Ω·cm ²)	C _{pl} [F]	R _{pl} (Ω·cm ²)	R _d (Ω·cm ²)	t (s)	L [H]	R _{ct} (Ω·cm ²)
1M	109.10	-9.76·10 ⁻⁶	938.0	3941.0	16.43	11884.0	913.40
4M	6.51	-44.03·10 ⁻⁶	120.70	94.48	0.35	804.30	57.13
Saturate	21.14	50.70·10 ⁻⁶	257.00	1417.0	37.03	---	---

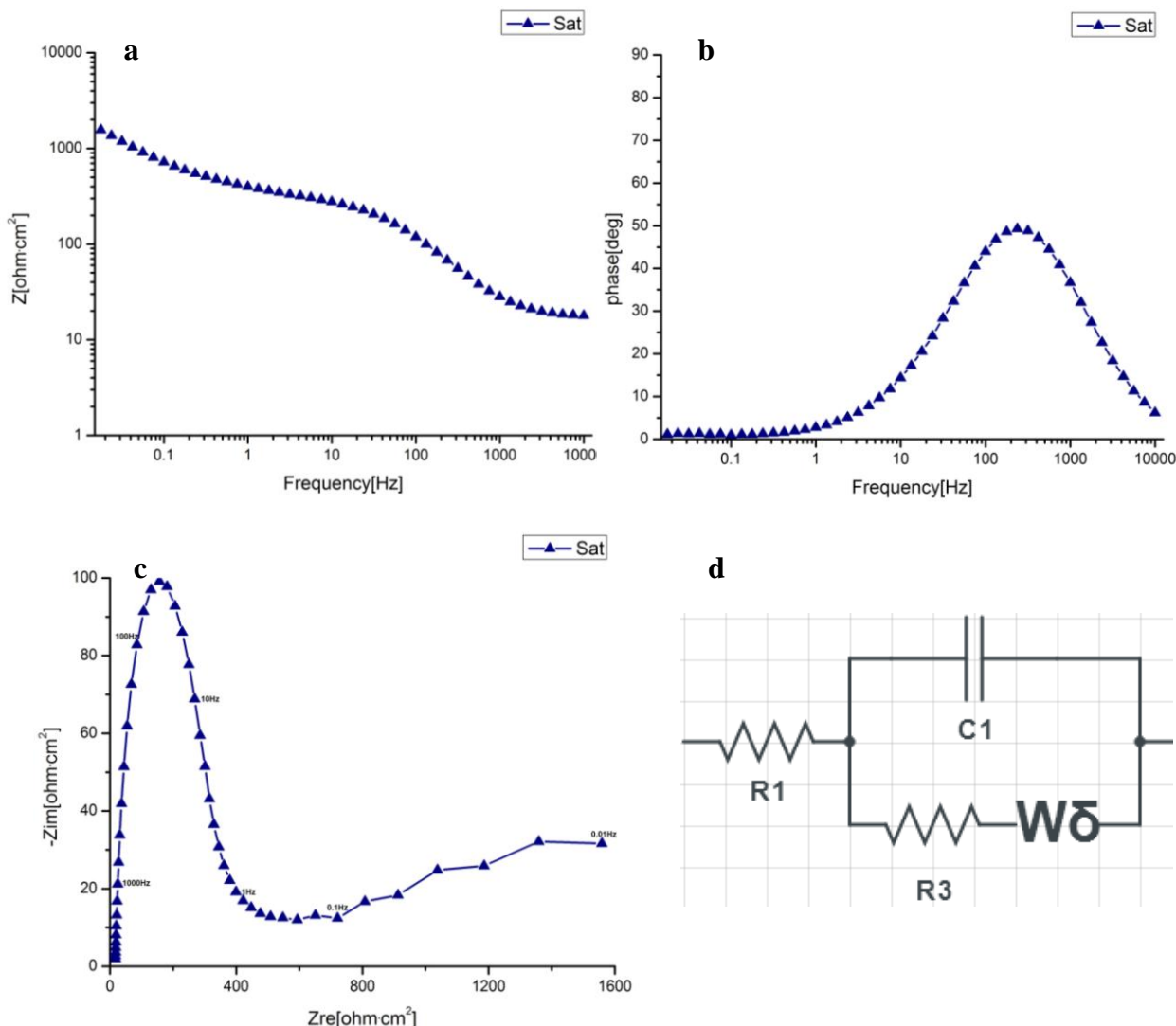


Figure 5. EIS spectra for Ti-2 in saturated NH₄Br solution at the transpassive area: (a)Bode diagram (b)Bode phase diagram (c)Nyquist diagram (d) Equivalent electrical circuit

The inductive coil represents the electrical activity during the anodic dissolution and propagation of the pits on the anodic surface. The EIS technique measures the activity on the surface and only active pits will be characterized as inductive coils. Generally, when the anodic dissolution is terminated, EIS cannot respond as a coil and only capacitors are detected.

When we compare the appearance of w^* we can conclude that high bromide concentration causes the inductive coil to appear at lower frequencies. In 1 M the peak exists at a frequency of 0.074 Hz and in 4 M the peak exists at a frequency of 0.023 Hz. This shift indicates a longer period for relaxation. It means that in 4 M solution the pit activity takes place over a longer period of time compared to 1 M solution, which results in severity of the pitting attack. The electrical equivalent circuit shows inductive coil acting in parallel with a single capacitor combined with Rtd element (Fig. 4d). The Rtd electrical element is identified in the Bode diagram by an increase in the ohmic resistance within the range of the lower frequencies. This indicates a diffusion control process that may be related

to the solid state diffusion process taking place during the passive film development when applying the anodic potential [24-26]. *t* value represents the period of time that the Rtd element remained dominant before the breakdown. It is clearly seen from Fig 4c and table 3 that the time (*t*) increases with decreasing bromide concentration, meaning that the thickness of the passive layer in 1 M ammonium bromide is greater compared to that in 4 M NH₄Br solution.

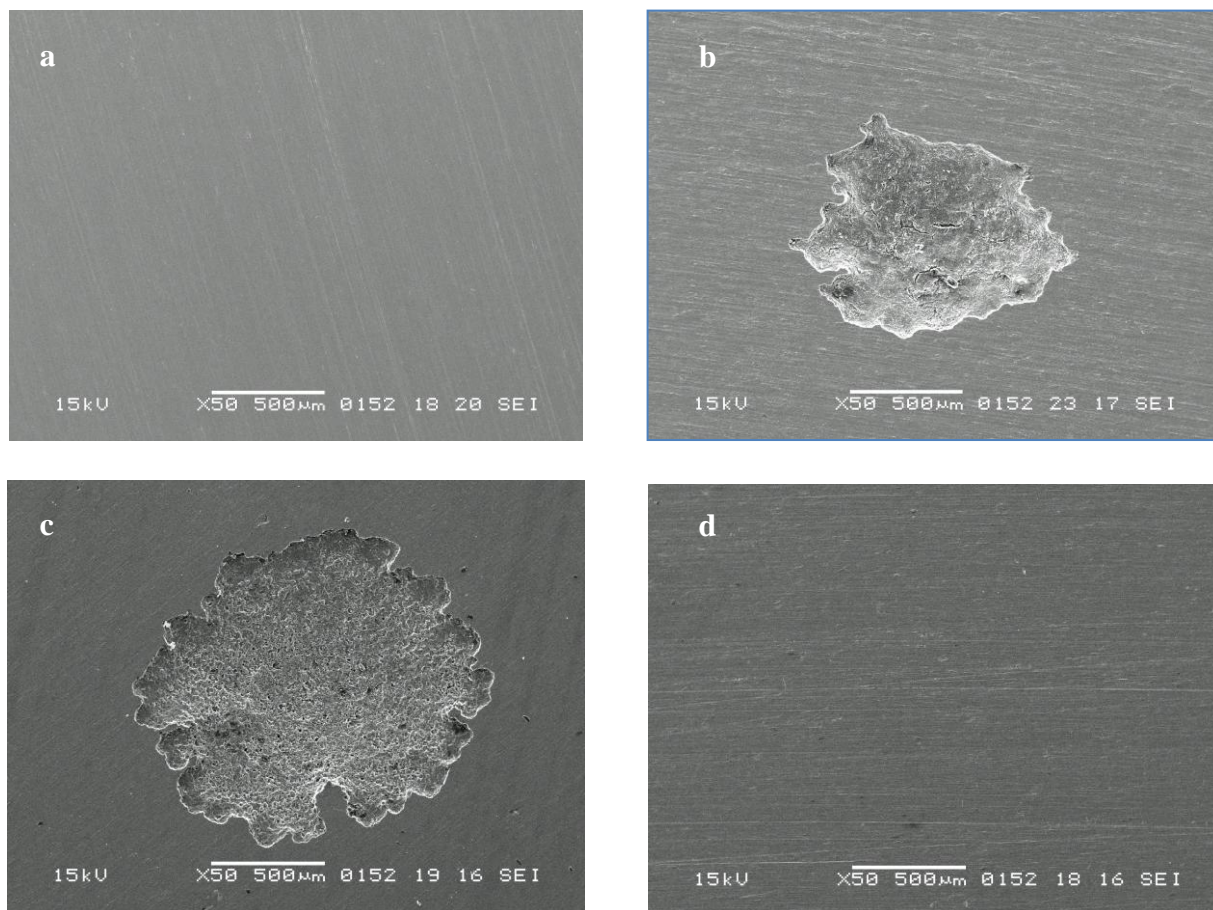


Figure 6. SEM observations for Ti-2 in NH₄Br solution in different concentrations: (a)reference sample (b) 1M (c)4M (d)saturated solution

When dealing with the saturated ammonium bromide solution, a significant change of behavior is observed when anodic potentials above the breakdown were applied, as presented in Fig. 5a-c. As is clearly seen, an inductive coil is not observed and the Rtd element remains dominant under low frequencies. This behavior indicates a stable passivity with no breakdown phenomenon.

When we want to calculate the relative permittivity in the case of a saturated solution we use the following equation. The capacitance *C* of plate capacitor of area *A* and distance *d* is expressed by the equation below:

$$C = \frac{\epsilon_r \cdot \epsilon_0 \cdot A}{d}$$

ϵ_r = relative permittivity of the dielectric material between the plates. From the literature, parameter d in the case of TiO_2 formation under 1.4 V vs. Ag/AgCl equals 8 nm [27]. As mentioned, the exposure area is given as $4.5 \cdot 10^{-4} \text{ m}^2$. In accordance with the equivalent electrical circuit, the capacitance is $50.70 \cdot 10^{-6}$ Farad (taken from Table 3). Given the above values, ϵ_r equals approximately 102. According to the literature, the typical range of values of ϵ_r for TiO_2 is between 85 and 173, depending on crystalline direction [28]. SEM observations in Fig. 6 show the surface morphology after exposure to different ammonium bromide solutions. It is clearly seen that after increasing the concentration from 1 M to 4 M the pitting has become more severe, but in the saturated solution the pitting attack cannot be identified. This finding supports the idea presented by the polarization analysis and EIS that no breakdown phenomenon can be detected under saturated NH_4Br solution.

4. CONCLUSIONS

1. Anomalous pitting sensitivity of titanium in ammonium bromide solutions was detected. Under saturation conditions pitting was not observed, even the anodic electrical field was above breakdown.
2. Under conditions of saturated ammonium bromide, cyclic anodic polarization does not show a positive hysteresis loop. Current increase, mainly related to bromine and oxygen formation, was recorded.
3. Pitting sensitivity was detected when the ammonium bromide content in the aqueous solution was up to about 4 M. EIS indicates the formation of anodically active pits by the appearance of an inductive loop.
4. Under transpassivity in saturated solution EIS shows an increase in resistance with time without an inductive element in the equivalent electrical circuits. This also supports the idea that breakdown phenomenon and pitting attack do not occur under saturation.

NOMENCLATURE:

L	inductor element related to the initiation of the pitting process
M	Molar
Qdl	metal double layer CPE capacitance (Farad)
Qpl	passive film CPE capacitance (Farad)
Rct	resistive component (ohm) of charge transfer
Rp	resistive component (ohm) of polarization
Rs	resistive component (ohm) of the solution
Rtd	resistive component (ohm) time dependent
ω^*	value of the frequency in minima of the inductive loop
τ	time of relaxation
ϵ_0	permittivity of air, $8.8541 \cdot 10^{-12}$ Farad / meter

ACKNOWLEDGEMENTS

The authors thank ICL Ltd. for the use of their electrochemical lab.

References

1. Kathy Wang, *Mater. Sci. Eng., A*, 213 (1996) 134- 137
2. J. Pan, D. Thierry and C. Leygraf, *Electrochim. Acta.* 41(1996) 1143-1 153
3. S´ergio Luiz de Assis, Stephan Wolynec, Isolda Costa, *Electrochim. Acta.* 51 (2006) 1815–1819
4. D. Itzhak, T. Greenberg, *Mater. Sci. Eng., A.* 302 (2001) 135–140.
5. Dimitra Sazou, Kyriaki Saltidou, Michael Pagitass, *Electrochim. Acta.* 76 (2012) 48-61.
6. J.L. Trompette , L. Massot, L. Arurault, S. Fontorbes, *Corros. Sci.* 53 (2011) 1262–1268.
7. I. Dugdale and J. B. Cotton, *Corros. Sci.* 4(1964) 397 – 411.
8. Shizhong Huo and Xiaoxiong Meng, *Corros. Sci.* 31(1990) 281-286.
9. T.R. Beck, *J. Electrochem. Soc.*. 120 (1973) 1310-1316.
10. Peng Yong-yi, Yin Zhrmin, Li San-hau, *Trans.Nonferrous Met. Soc.Chaina.* 15(2005) 1226-1230.
11. Cao Chu-nam, Wang Jia, Lin Harchao, *Journal of CSCP.* 9(1989)261-270
12. Keddam M, Kuntz C, Takenouti H, *Electrochim. Acta.* 42(1997)87-97
13. Conde A, de Damborenea J. *Electrochim. Acta.* 43(1998)849-860
14. C. M. A. Brett, *J. Appl. Electrochem.*. 20 (1990) 1000-1003.
15. C. Madore and D. Landolt., *J. Micromech. Microeng.* 7 (1997) 270–275
16. O. Çakır, A. Yardımeden, T. Ozben, E. Kilickap, *Journal of Achievements in Materials and Manufacturing Engineering.* 25 (2007) 99-102.
17. F. El-Taib Heakal, Kh.A. Awad , *Int. J. Electrochem. Sci.* 6 (2011) 6483 – 6502
18. Ruihua Li, Zhanpeng Jiang, Fengen Chen , Hongwei Yang, Yuntao Guan , *J. Mol. Struct.* 707 (2004) 83-88
19. E. Blasco-Tamarit, A. Igual-Mun˜oz, J. Garcı’a Anto’n,D. Garcı’a-Garci’a, *Corros. Sci.* 49 (2007) 1000–1026.
20. Anelise Marlene Schmidt, Denise Schermann Azambuja , *Materials Research*, 9(2006) 387-392.
21. S.P. Trasatti, , E. Sivieri, *Materials Chemistry and Physics.* 83 (2004) 367–372.
22. J.R. Ambrose, J. Kruger, *Corros. Sci.*, 8 (1968) 119 – 124.
23. Y. Shterenberg, H.Straze and D.Itzhak, *Materials Science Forum.* 126 (1993) 753-756
24. H. Sakly, R.mlika, I.Bonnamour, F.Aouni, H.Ben Ouada and N.Jaffrezic Renault, *Electrochim. Acta* .52(2007) 3697-3703.
25. M.C. Lefebvre, B.E. Conway, *J. Electroanal. Chem.* 480 (2000) 34–45
26. Vadim F. Lvovich, Matthew F. Smiechowski , *Electrochim. Acta.* 51 (2006) 1487–1496
27. Aikaterini G.Mantzila, Mamas I. Prodromidis , *Electrochim. Acta.* 51 (2006) 3537-3542
28. Obert G. Breckenridge and William R. Hoslfr. *Phys. Rev.* 91 (1953) 794-802.